Appendix. Supplementary Information

Preparation of bottom-up graphene oxide using citric acid and tannic acid, and its application as a filler for polypropylene nanocomposites

Huiseob Shin[1], Min-Young Lim[1], Jinwoo Oh[2], Yonghoon Lee [3], and Jong-Chan Lee[1,*]

[1]School of Chemical and Biological Engineering and Institute of Chemical Processes, Seoul National University, 1 Gwanak-ro, Gwanak-gu, Seoul, 08826, Republic of Korea

[2]Photo-Electronic Hybrids Research Center, Korea Institute of Science and Technology (KIST), 5. Hwarang-ro 14-gil, Seongbuk-gu, Seoul, 02792, Republic of Korea

[3]Chemical Pilot Bldg., S-OIL TS&D Center, 31 Magokjungang 8-ro 1-gil, Gangseo-gu, Seoul, 07793, Korea

Correspondence to: J.-C. Lee (E-mail: jongchan@snu.ac.kr, Fax: +82-2-880-8899, Tel: +82-2-880-7070)

Figure S1 FT-IR spectrum of BGOs prepared by different weight ratio of CA/TA.

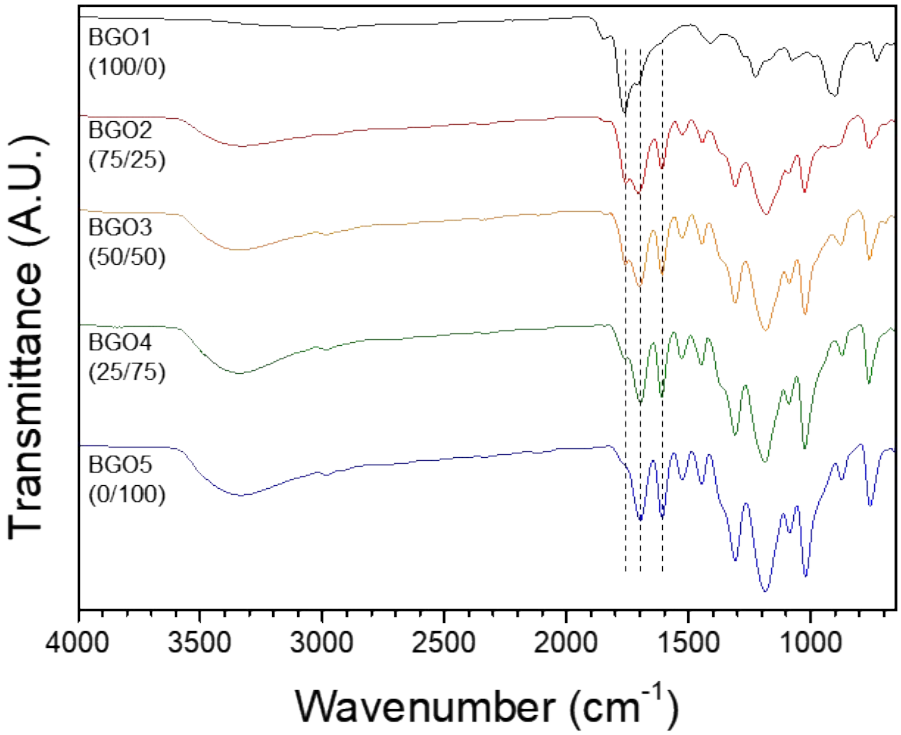

Figure S2 TEM images of (a) BGO1, (b) BGO2, (c) BGO3, (d) BGO4 and (e) BGO5.

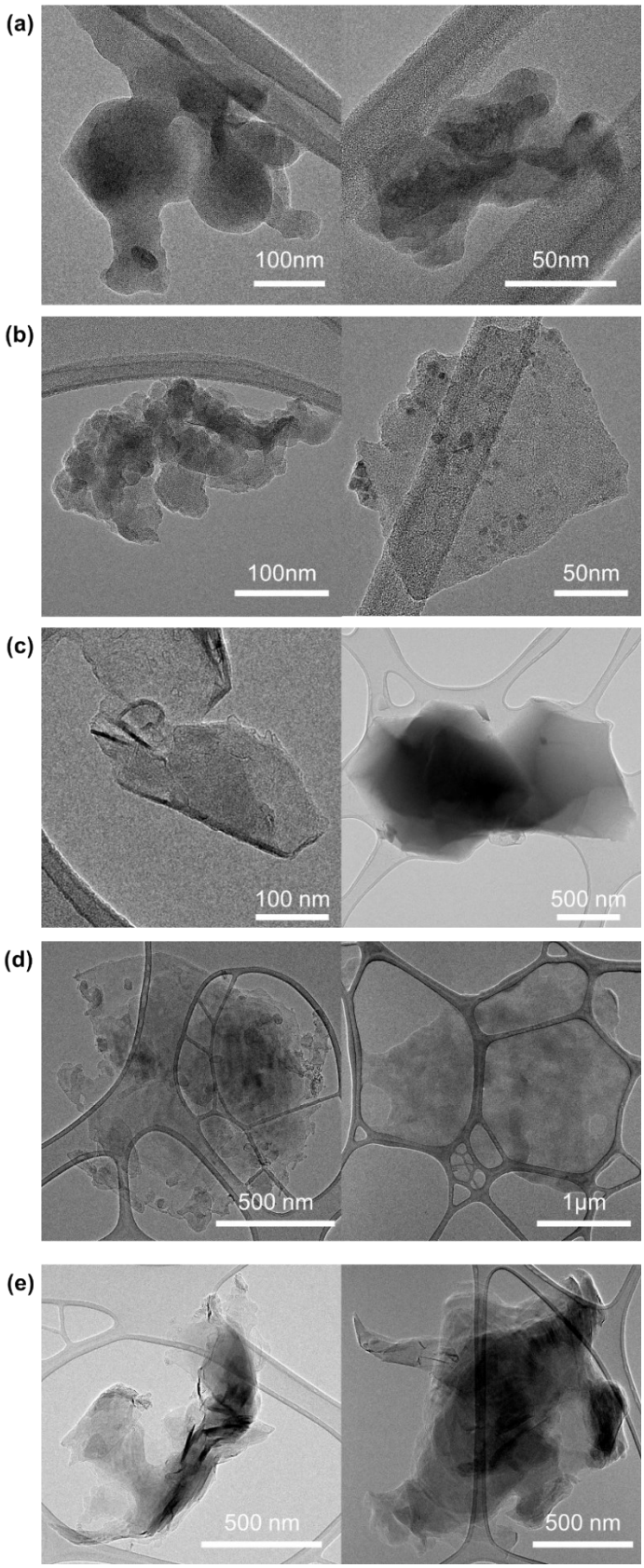

Figure S3 TEM images, AFM image, and height profile of (a) GO and (b) CGO.

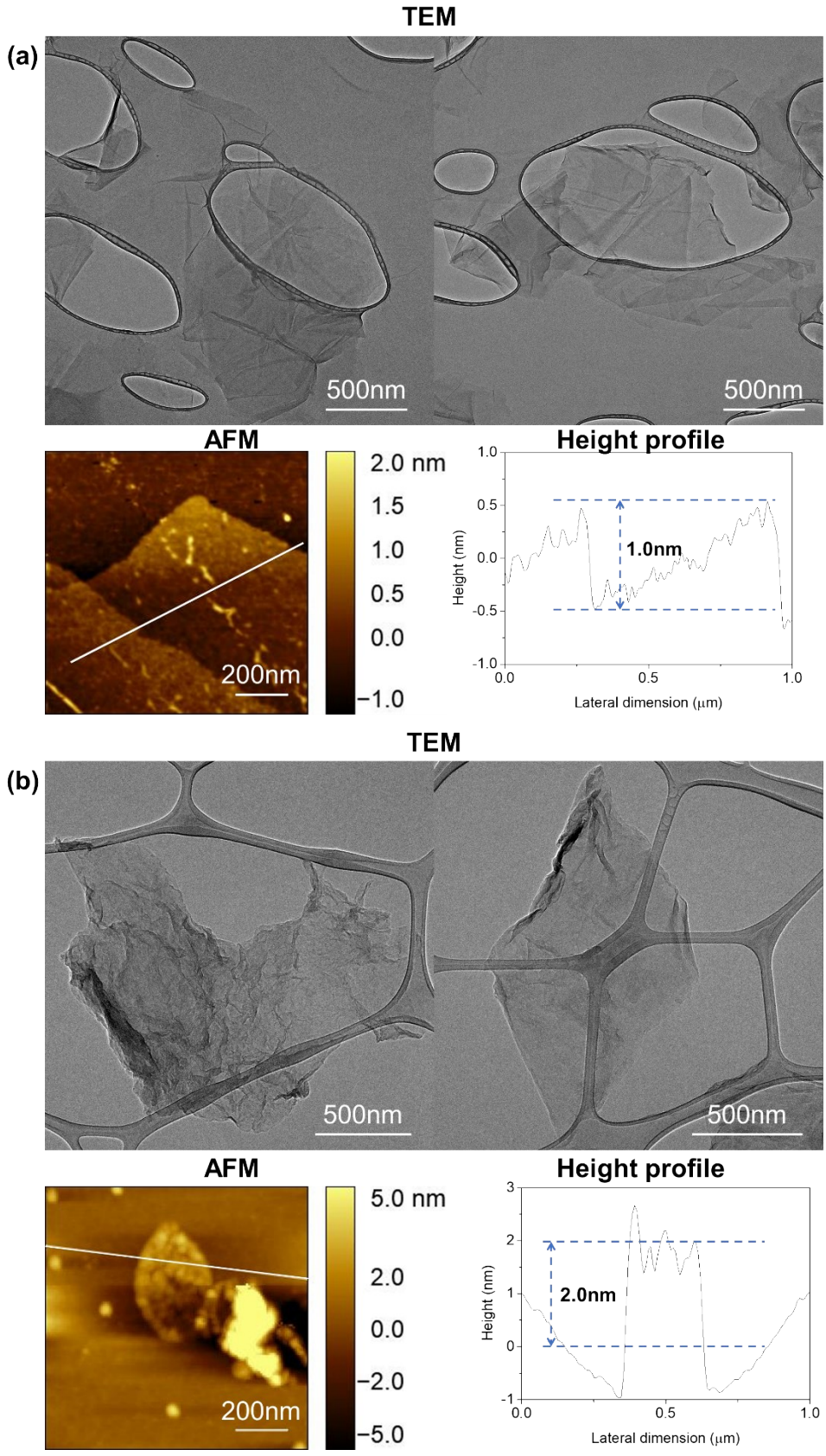

Figure S4 (a) XPS wide scan spectrum of BGO3 and CBGO3, (b) XPS C1s scan of BGO3, and (c) XPS C1s scan of CBGO3.

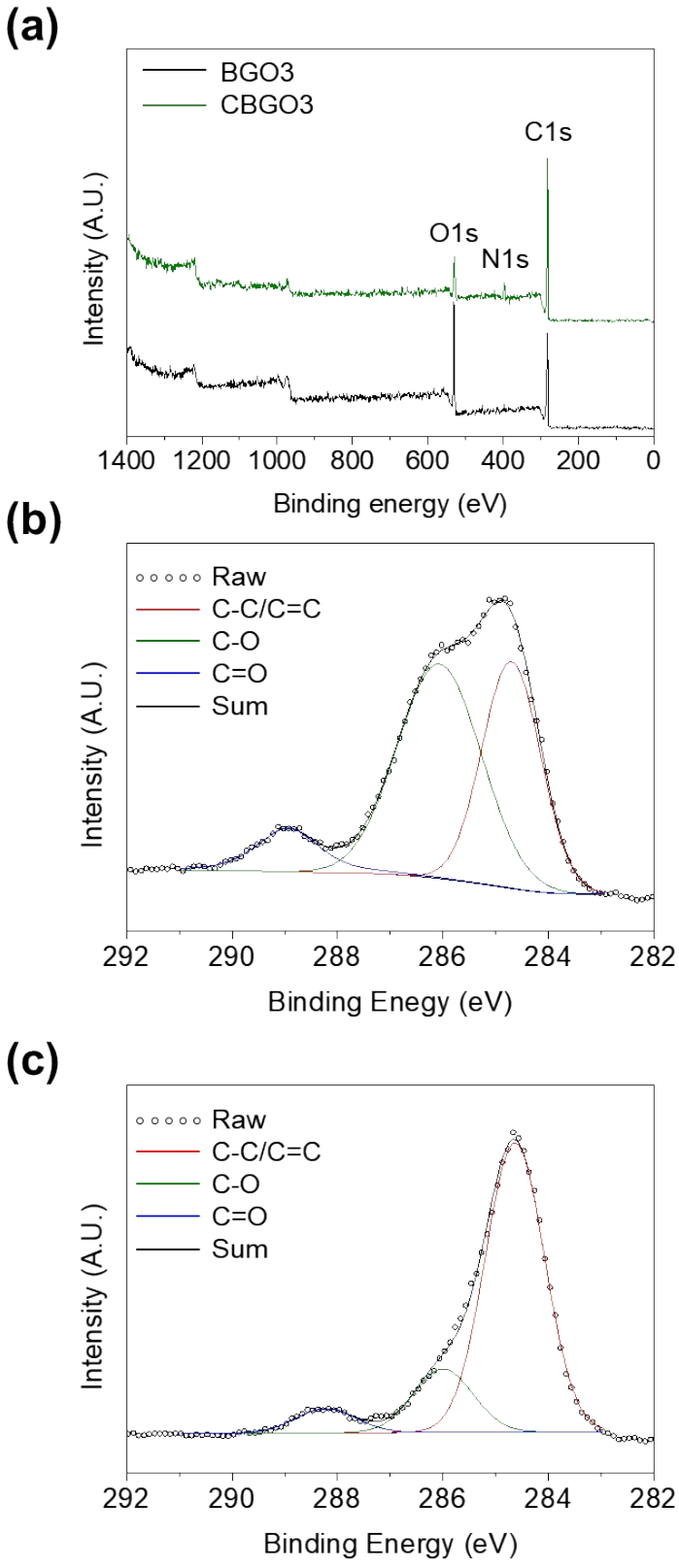

Figure S5 Tensile test results of PP/BGO3 nanocomposites. (a) Tensile strength, (b) Young's modulus, (c) elongation at break, and (d) representative strain-stress curves.

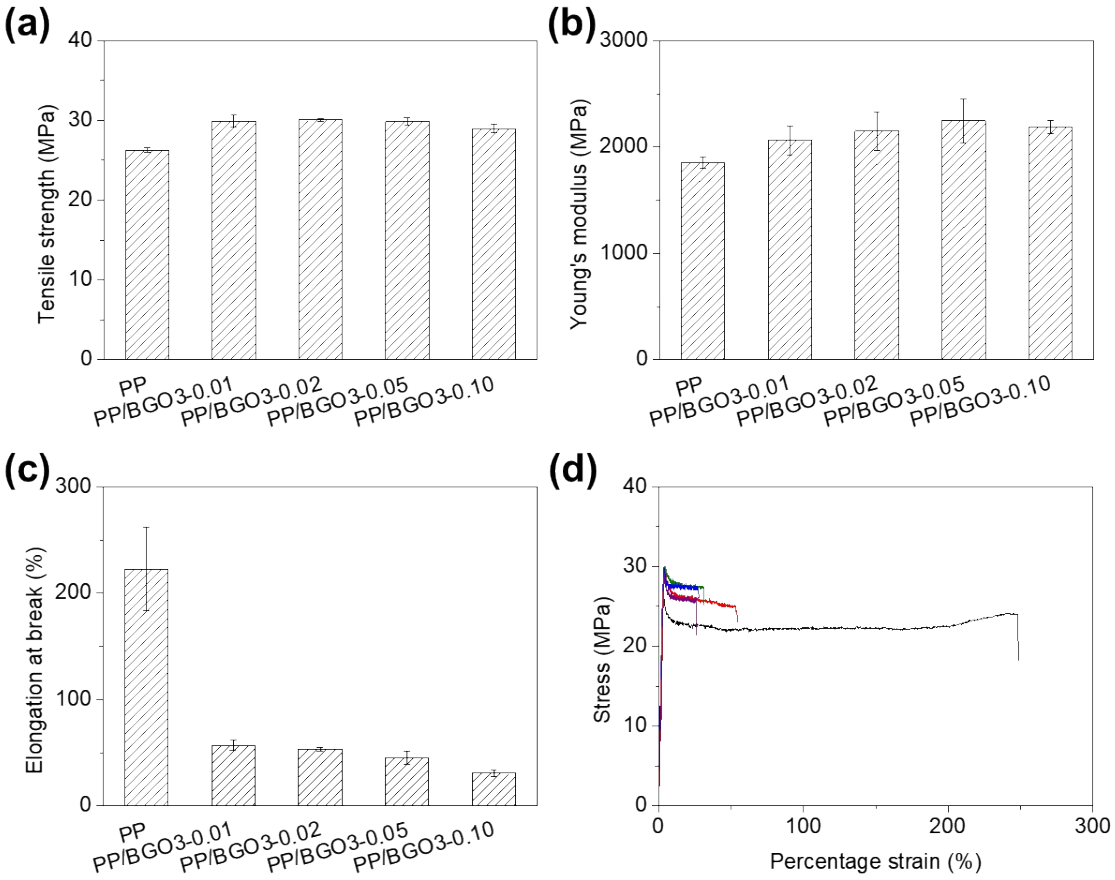

Figure S6 Tensile test results of PP/CBGO3 nanocomposites. (a) Tensile strength, (b) Young's modulus, (c) elongation at break, and (d) representative strain-stress curves.

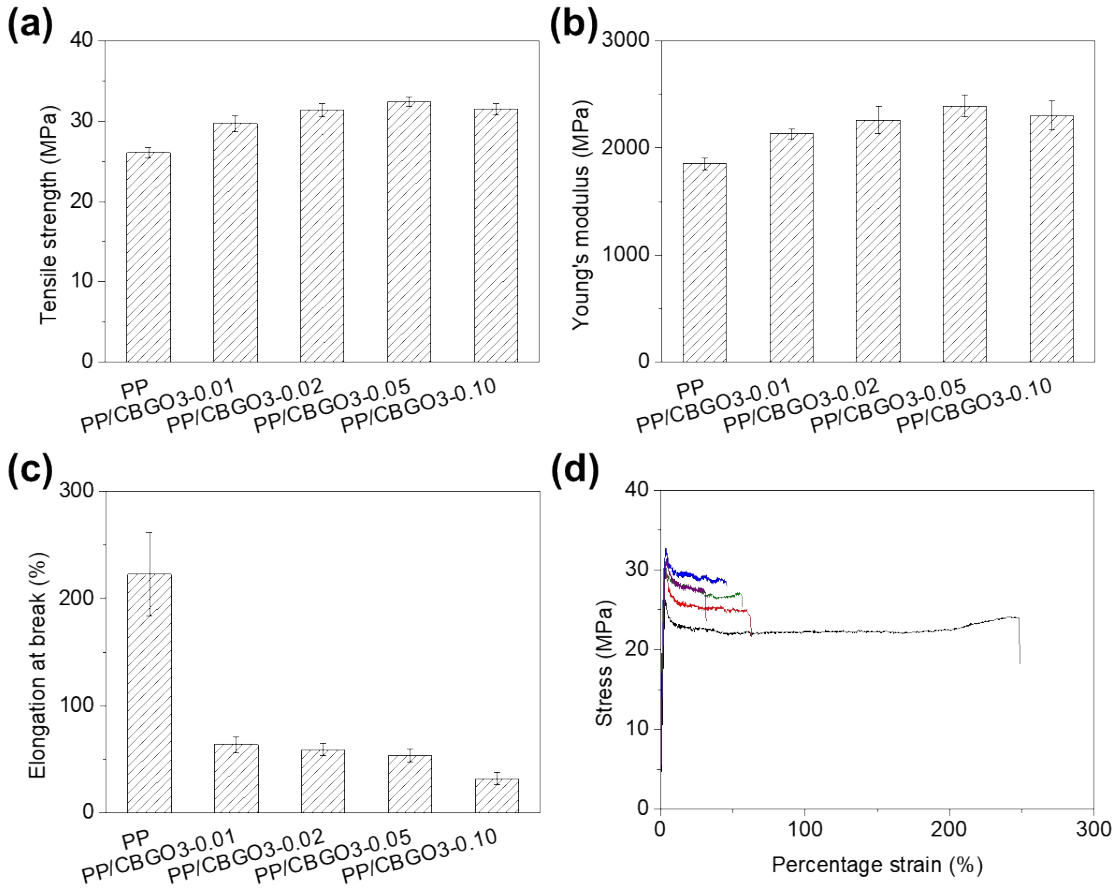

Figure S7 Tensile test results of PP/GO nanocomposites. (a) Tensile strength, (b) Young's modulus, (c) elongation at break, and (d) representative strain-stress curves.

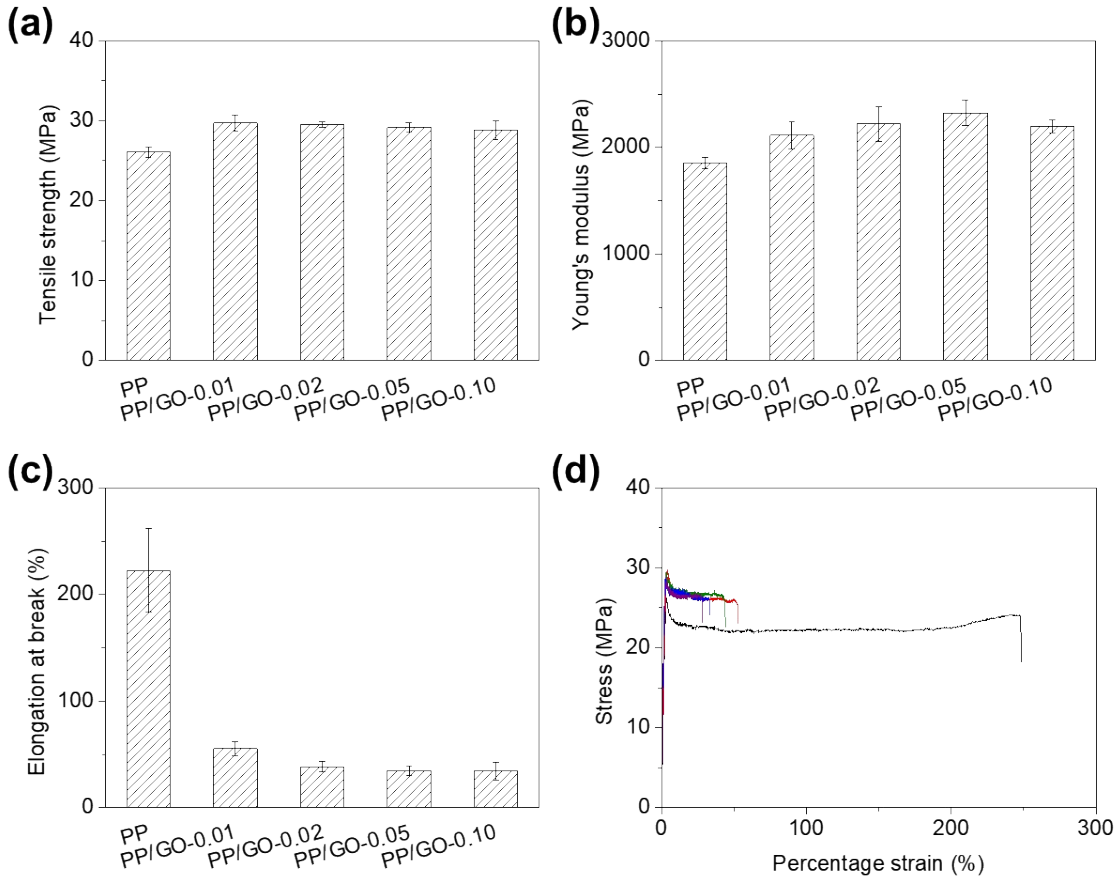

Figure S8 Tensile test results of PP/CGO nanocomposites. (a) Tensile strength, (b) Young's modulus, (c) elongation at break, and (d) representative strain-stress curves.

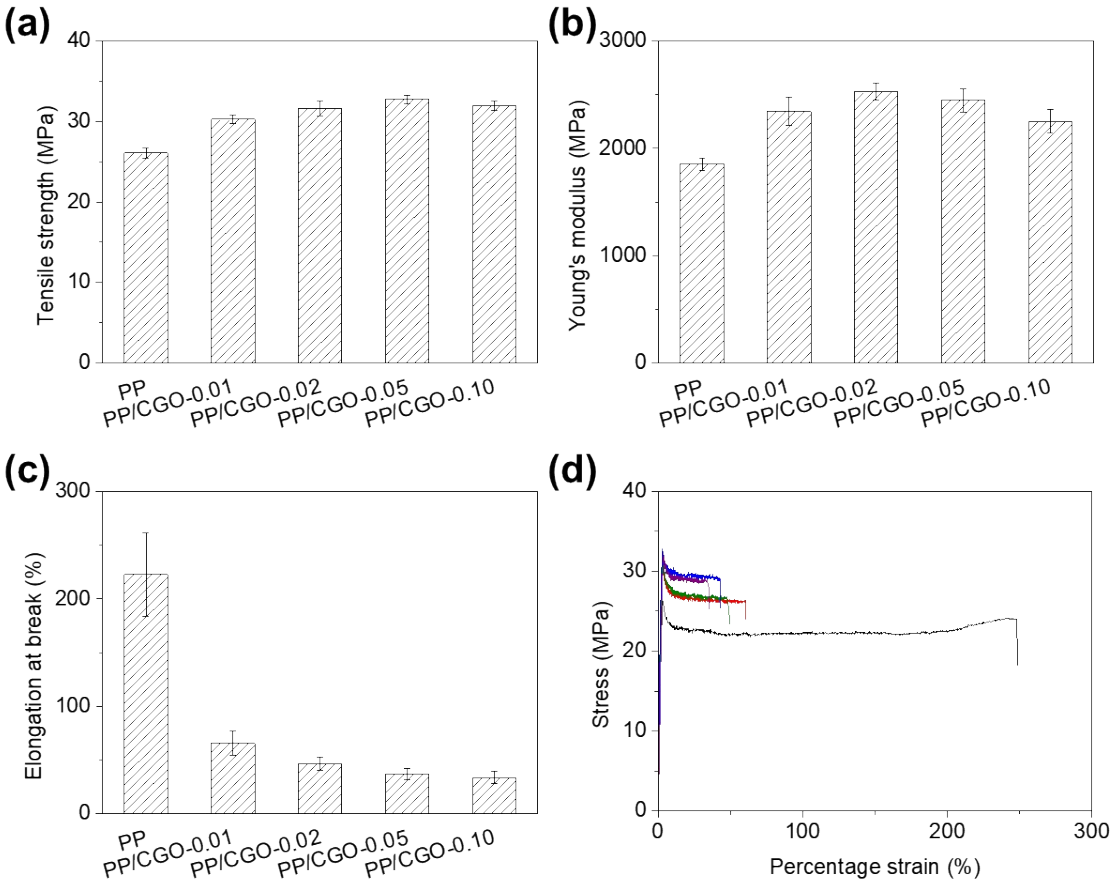

Figure S9 (a) TGA curves, (b) XRD patterns, (c) DSC cooling curves, and (d) DSC heating curves of pristine PP and PP nanocomposites containing 0.05 wt% of fillers.

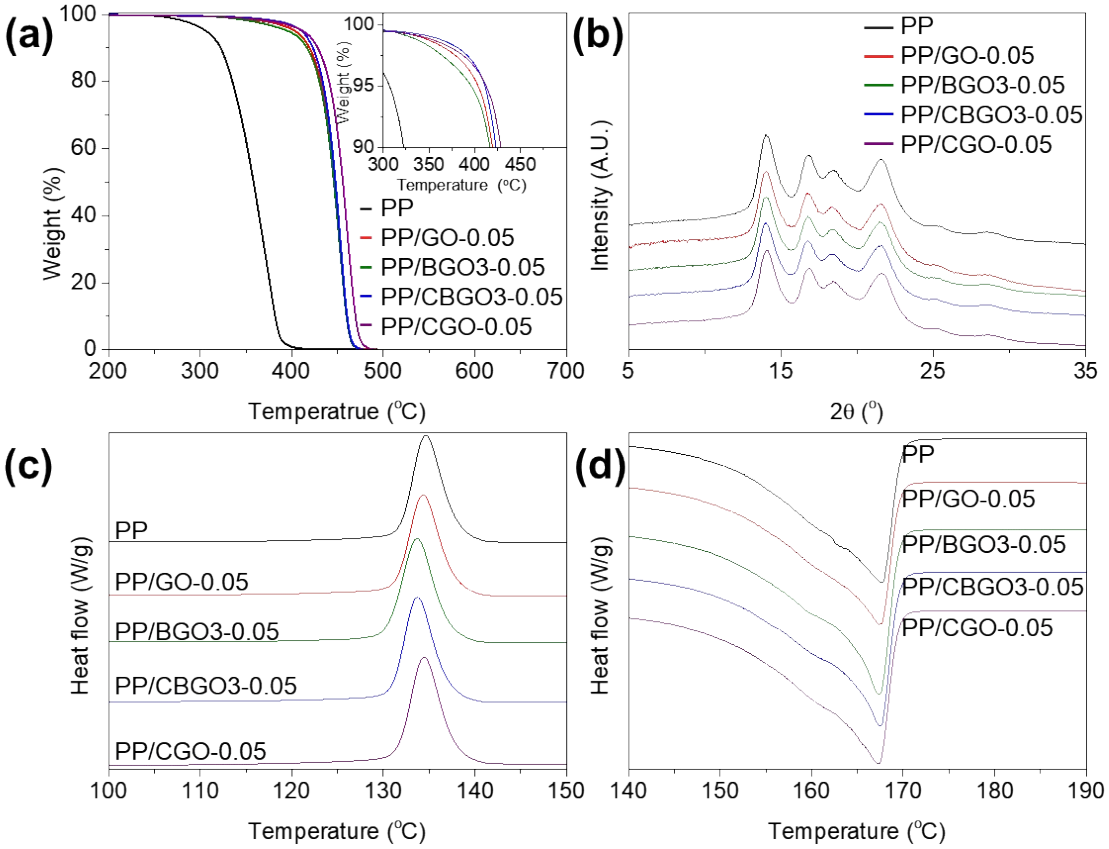

Figure S10 TGA curves of PP nanocomposites. (a) PP/BGO3, (b) PP/CBGO3, (c) PP/GO and (d) PP/CGO nanocomposites.

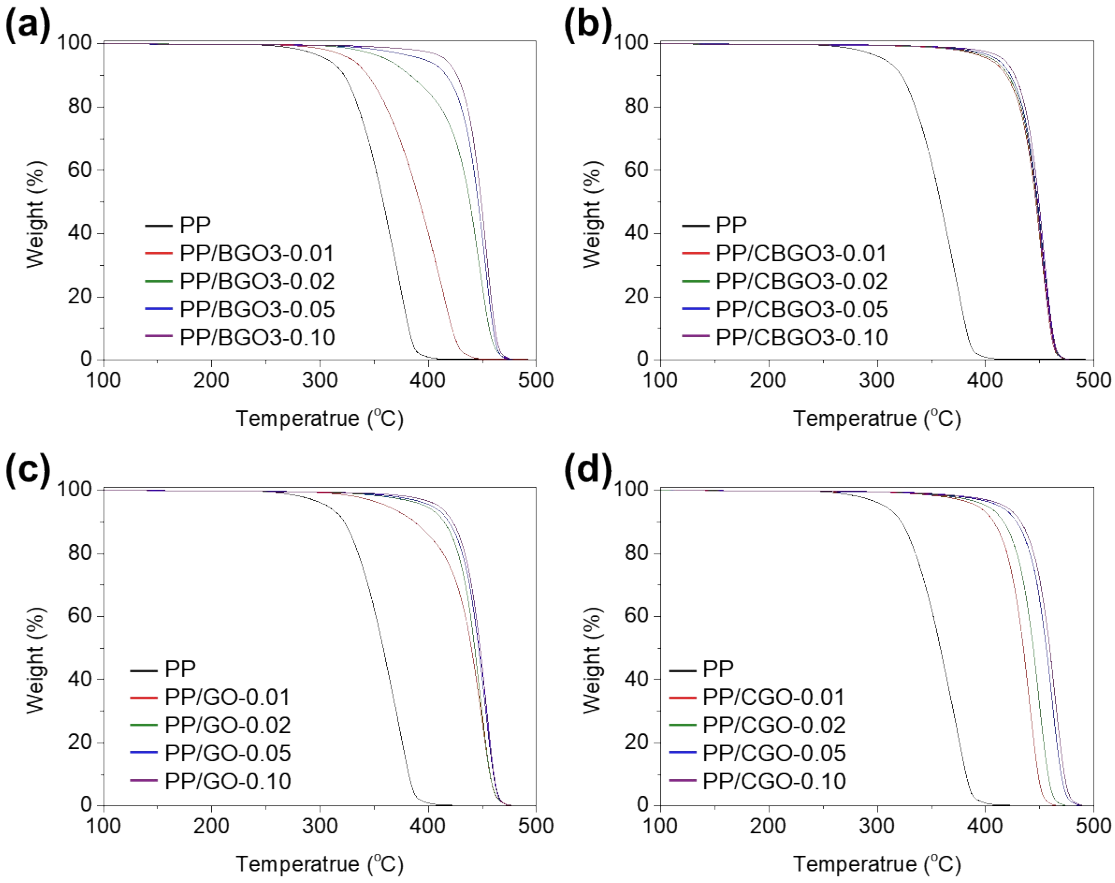

Figure S 11 XRD patterns of PP nanocomposites. (a) PP/BGO, (b) PP/CBGO3, (c) PP/GO, and (d) PP/CGO nanocomposites.

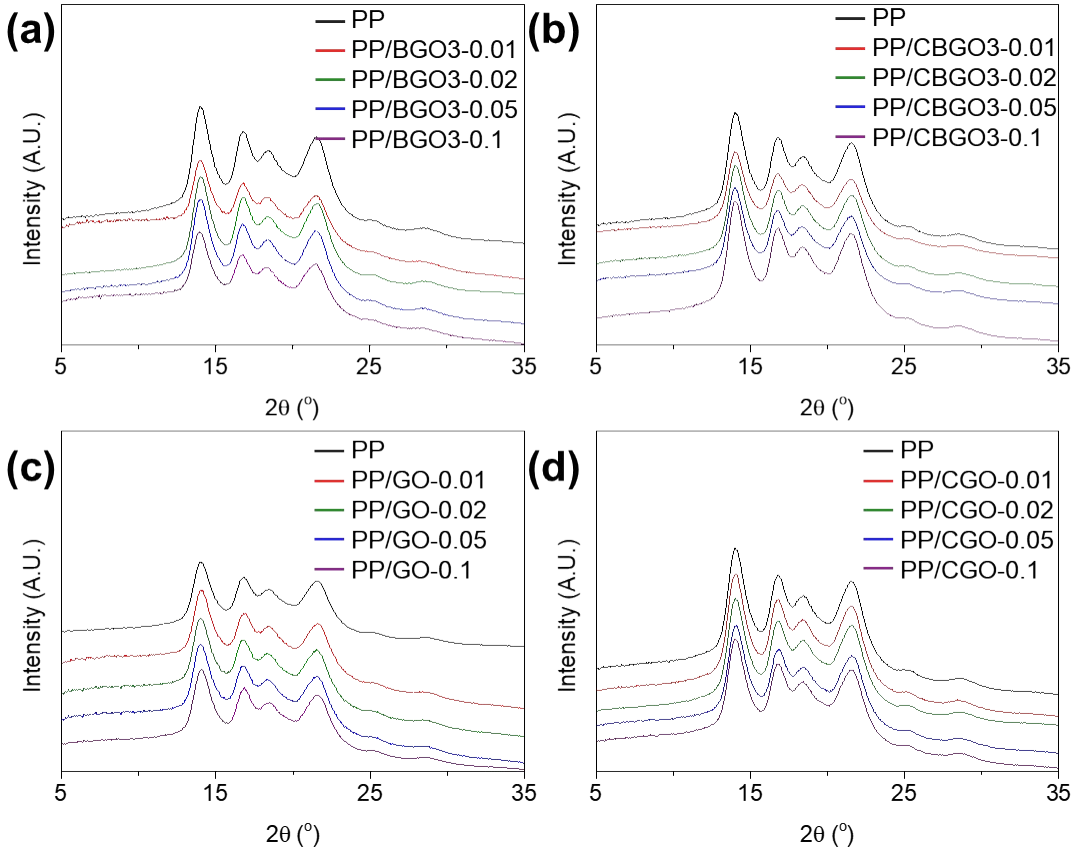

Figure S 12 DSC results of PP nanocomposites. (a) PP/BGO3 nanocomposites, (b) PP/CBGO3 nanocomposites, (c) PP/GO nanocomposites, and (d) PP/CGO nanocomposites.

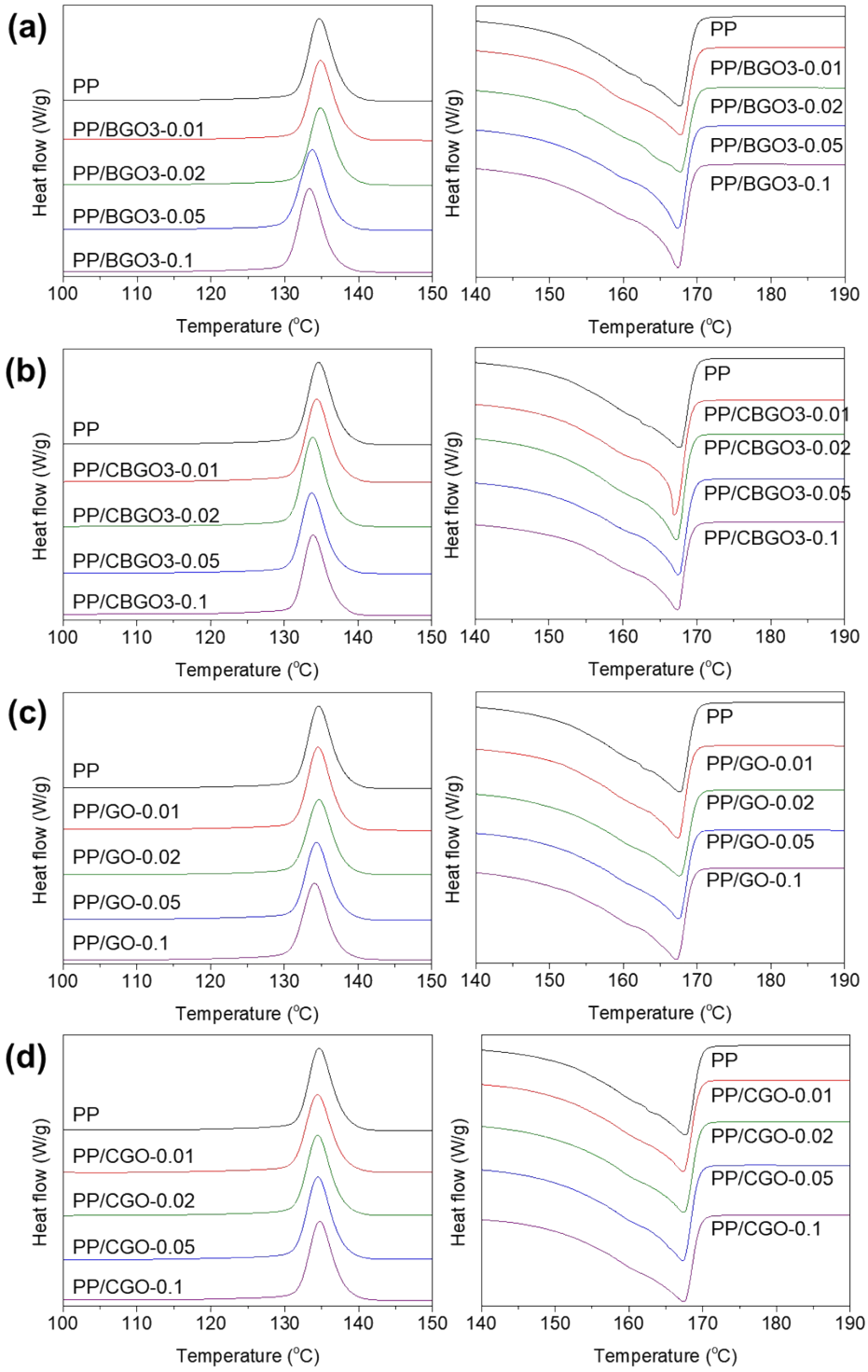

Figure S13 TEM images of fillers in PP nanocomposites containing 0.05 wt% of fillers. (a) BGO3. (b) CBGO3. (c) GO. (d) CGO.

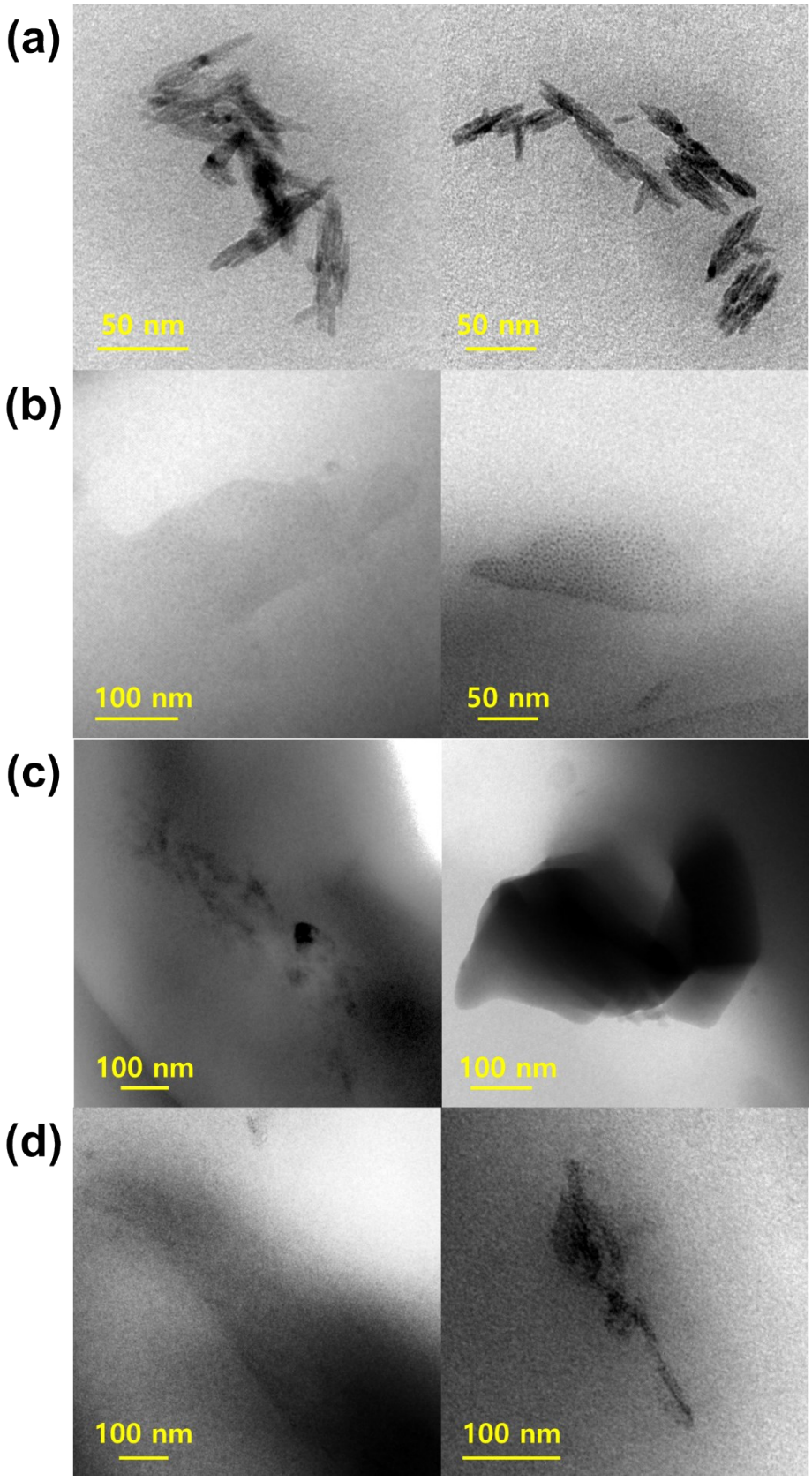

Figure S 14 DMA results of pristine PP and PP nanocomposites. (a) Storage modulus values. (b) Loss modulus values. (c) Tan δ values.

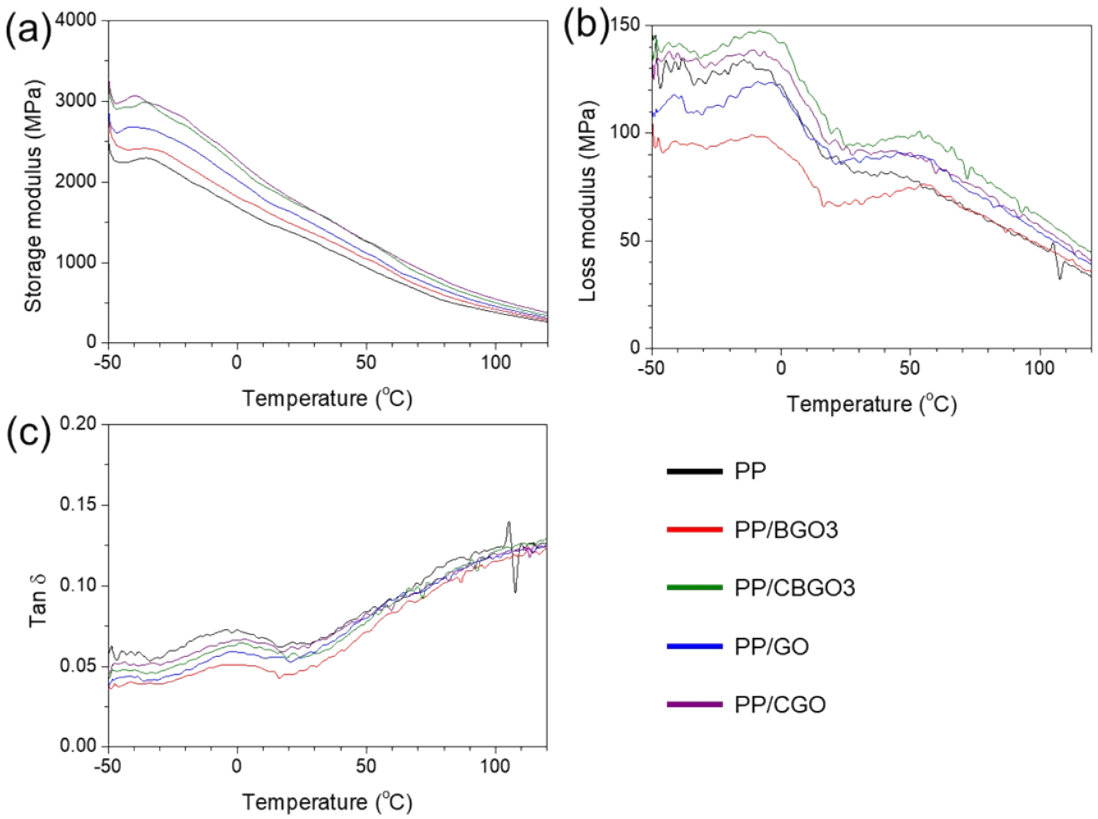

Table S1 Elemental analysis result of BGOs and CBGO3.

Sample	CA/TA[a]	Content (wt%)			
		C	H	O	N
BGO1	100/0	53.3	4.1	42.5	0.0
BGO2	75/25	55.9	4.0	40.1	0.0
BGO3	50/50	51.7	3.9	44.4	0.0
BGO4	25/75	52.8	4.2	43.0	0.0
BGO5	0/100	51.4	3.9	44.7	0.0
CBGO3	-	55.2	4.8	39.4	0.6

[a] The weight ratio of CA/TA used for the preparation of BGO.

Table S 2 Mechanical properties and Thermal degradation temperature for 5 wt% loss ($T_{d,5}$) of pristine PP and PP nanocomposites.

Sample	Tensile strength (MPa)	Young's modulus (MPa)	Elongation at break (%)	$T_{d,5}$ (°C)
PP	26.1±0.3	1853.4±57.1	222.7±38.8	307.0
PP/BGO3-0.01	29.9±0.7	2061.0±137.6	56.9±4.6	329.7
PP/BGO3-0.02	30.1±0.1	2152.2±180.1	53.2±1.8	362.4
PP/BGO3-0.05	29.9±0.5	2247.5±208.4	45.0±6.3	396.4
PP/BGO3-0.10	29.0±0.5	2186.2±62.1	30.7±3.2	416.3
PP/CBGO3-0.01	29.7±1.0	2132.3±49.7	63.6±7.5	403.6
PP/CBGO3-0.02	31.4±0.8	2260.6±124.6	58.8±5.6	407.2
PP/CBGO3-0.05	32.4±0.6	2392.5±103.6	53.2±6.4	411.2
PP/CBGO3-0.10	31.5±0.7	2302.3±136.4	31.7±5.5	416.9
PP/GO-0.01	29.7±1.0	2113.8±130.6	55.5±6.6	362.0
PP/GO-0.02	29.5±0.4	2219.3±166.8	38.3±4.8	397.4
PP/GO-0.05	29.1±0.6	2323.7±119.4	34.7±4.0	403.3
PP/GO-0.10	28.8±1.2	2199.3±60.6	34.4±8.2	409.7
PP/CGO-0.01	30.3±0.5	2344.5±133.1	65.4±11.6	392.5
PP/CGO-0.02	31.6±1.0	2526.1±78.4	46.3±5.9	401.2
PP/CGO-0.05	32.8±0.5	2448.2±109.7	36.3±5.4	412.7
PP/CGO-0.10	32.0±0.5	2251.6±107.0	33.3±5.5	417.6

Table S 3 DSC results of pristine PP and PP nanocomposites.

Sample	Cooling			Heating		
	Onset temperature (^{o}C)	Peak temperature (^{o}C)	Heat of crystallization (J/g)	Onset temperature (^{o}C)	Peak temperature (^{o}C)	Heat of melting (J/g)
PP	138.2	134.7	92.1	152.8	167.6	87.3
PP/BGO3-0.01	138.3	134.8	87.6	154.4	167.7	86.2
PP/BGO3-0.02	138.3	134.9	86.0	152.9	167.6	84.0
PP/BGO3-0.05	137.3	133.7	92.5	159.8	167.3	89.2
PP/BGO3-0.1	136.8	133.4	90.3	160.4	167.4	87.8
PP/CBGO3-0.01	137.9	134.4	92.6	165.1	166.9	87.2
PP/CBGO3-0.02	137.4	133.9	98.8	158.9	167.2	94.5
PP/CBGO3-0.05	137.2	133.8	89.1	159.5	167.4	84.0
PP/CBGO3-0.1	137.4	133.9	83.8	158.3	167.4	77.2
PP/GO-0.01	138.1	134.6	91.8	155.7	167.4	86.7
PP/GO-0.02	138.2	134.7	89.2	153.2	167.6	86.7
PP/GO-0.05	137.9	134.4	89.0	156.3	167.3	84.7
PP/GO-0.1	137.6	134.1	88.1	155.7	167.1	87.6
PP/CGO-0.01	138.1	134.4	91.3	155.3	167.3	88.3
PP/CGO-0.02	137.9	134.4	91.0	155.0	167.4	87.6
PP/CGO-0.05	138.0	134.5	93.5	155.4	167.3	88.5
PP/CGO-0.1	138.2	134.7	87.0	153.8	167.3	83.9